

- [21] Y. Li, C. L. Cahill, P. C. Burns, *Chem. Mater.* **2001**, *13*, 4026–4031.  
 [22] R. E. Sykora, K. M. Ok, P. S. Halasyamani, T. E. Albrecht-Schmitt, *J. Am. Chem. Soc.* **2002**, *124*, 1951–1957.  
 [23] G. M. Sheldrick, SHELXTL PC, Version 5.0, Siemens Analytical X-Ray Instruments, Inc., Madison, WI **1994**.

## A $C_{2v}$ -Symmetric Barbaralane\*\*

Markus Reiher\* and Barbara Kirchner\*

Barbaralane **1** (see Figure 1) is one of the fluxional molecules that undergo a degenerate Cope rearrangement. It was proposed by W. von E. Doering that the activation barrier of the Cope rearrangement is lower in **1** than in 3,4-homotropilidene<sup>[1]</sup> as barbaralane is already fixed in the appropriate boat conformation by a bridge between the two corner atoms C1 and C5. If this activation barrier were lowered even further, one might arrive at a symmetrical and therefore homoaromatic, biradical, or biradicaloid ground state. The objective is to transform the double-minimum system **1** into one with a single minimum by increasing the symmetry, that is, by changing from a  $C_s$ - to a more symmetric ( $C_{2v}$ ) ground-state structure. Much effort was made to find a symmetrical ground-state structure by studying various derivatives experimentally and theoretically (e.g., semiempirical MO calculations<sup>[2,3]</sup>). The most valuable overview was given by Quast et al.<sup>[4]</sup> Additional reviews can be found in refs. [1,5,6] and references cited therein. These investigations yielded the following results: At the C2 and the C6 positions only electron-withdrawing groups that are  $\pi$  acceptors lower the barrier. Aryl groups at these positions are most effective. The same  $\pi$ -acceptor substituent causes only slight changes at the C3 and C7 positions.

From the possible derivatives of **1** we chose to replace the 2,4,6,8-positions of barbaralane by heteroatoms (Figure 1). The use of nitrogen or oxygen has been suggested.<sup>[4]</sup> A derivative of 2,4,6,8-tetraazabarbaralane (**2a**) was studied before; it does not give a symmetrical ground state (**2b** or **2c**), but the activation barrier of the Cope rearrangement is

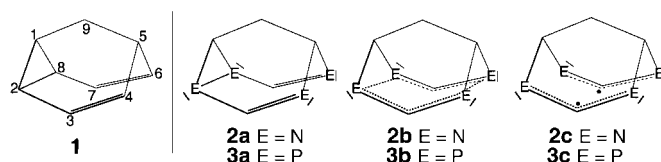


Figure 1. Barbaralane **1** and some possible heterobarbaralanes **2**.

lowered relative to that of the carbon analogue.<sup>[7]</sup> This is in accordance with the observation of Schnieders et al., who found lowering of the Cope barrier in a 2,6-diazasemibullvalene derivative<sup>[8]</sup> relative to the carbon analogue. A logical consequence from these studies is replacement of carbon by phosphorus atoms, which can be achieved by replacing a CH moiety with a P atom as they are valence isoelectronic. Phosphorus produces smaller bond angles than carbon, and this can affect the stability of cyclic compounds.<sup>[9]</sup> Hence, we proposed to study the novel compound 2,4,6,8-tetraphosphabarbaralane (**3**), and we also re-examined parent barbaralane (**1**) and 2,4,6,8-tetraazabarbaralane (**2a**).

Figure 2 shows the three molecules with selected bond lengths, as obtained from DFT geometry optimizations (see Methods of Calculation). The most striking feature is that **3**

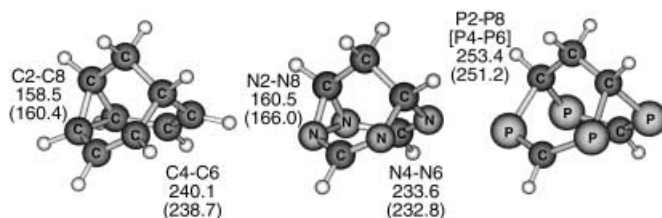


Figure 2. B3LYP/TZVPP optimized structures of barbaralane (left), tetraazabarbaralane (middle), and tetraphosphabarbaralane (right). Distances are given in picometers (BP86/TZVPP values in parentheses).

clearly has  $C_{2v}$  symmetry. Frequency analysis of this geometrical arrangement indeed confirmed a minimum structure.

The overall agreement between the B3LYP and BP86 (in parentheses) bond lengths is very good: deviations are less than 2 pm (with the exception of the N2–N8 bond length, for which the BP86 value deviates by 5.5 pm from the B3LYP value). Therefore, in the following discussion we concentrate on B3LYP/TZVPP data. Closer inspection reveals that the C1–C9–C5 substructure (1,5-bridge) is almost identical in all the barbaralanes (e.g., the C9–C5 distances vary between 154.7 and 152.1 pm). Deviations are within 2.6 pm and are due to bond shortening in the heterobarbaralanes compared to the parent barbaralane. The two bonds building this bridge are of almost identical length in **1** and **2a**, and completely identical in **3**. Whereas all nitrogen–carbon distances are contracted by about 5 pm compared to the equivalent C–C distances in parent barbaralane, the N2–N8 distance is longer and the N4–N6 distance is shorter than the equivalent C–C distance, and this results in a molecule more symmetrical than the parent barbaralane.

In **3** we found for every interatomic distance involving phosphorus a bond elongation by more than 25 pm compared to the parent barbaralane **1**. Since the P2[4]–P8[6] distances (253.4 pm) are larger than the typical  $\sigma$  bond lengths in  $P_6$ <sup>[10]</sup>

[\*] Dr. M. Reiher  
 Lehrstuhl für Theoretische Chemie  
 Universität Erlangen-Nürnberg  
 Egerlandstraße 3, 91058 Erlangen (Germany)  
 Fax: (+49)91318527736  
 E-mail: markus.reiher@chemie.uni-erlangen.de

Dr. B. Kirchner  
 Physikalisch-Chemisches Institut  
 Universität Zürich  
 Winterthurerstrasse 190, 8057 Zürich (Switzerland)  
 Fax: (+41)635 6838  
 E-mail: kirchner@pci.unizh.ch

[\*\*] The authors thank Prof. B. A. Hess (Erlangen), Prof. J. Hutter (Zürich), J. Neugebauer (Erlangen), and D. Dath (Freiburg). B.K. especially thanks Prof. K. Müllen (Mainz) for inspiring lectures during her student days, and the Deutsche Forschungsgemeinschaft for a generous Forschungsstipendium.

(236 and 222 pm) and  $P_4$  (222 pm)<sup>[11]</sup> (all distances from B3LYP/TZVP calculations), we assume we are not dealing with such a bond type. This is confirmed by consideration of the HOMOs and the electron localization function (ELF; see below). Note that for some substituted semibullvalenes it was previously observed that shortening of the 1,5-bridge is accompanied by opening of the cyclopropane ring,<sup>[4]</sup> as can be seen in tetraphosphabarbaralane in Figure 2. Thus, the symmetrical phosphabarbaralane is achieved by two geometrical changes: 1) the C1-C9-C5 bridge is shortened, and 2) the angle at C1 is enlarged, that is, the C2-C8 bond is elongated.

Unrestricted B3LYP/TZVP calculations on **3** showed that the energy of the lowest lying triplet state (biradical) was more than 100 kJ mol<sup>-1</sup> higher than that of the lowest lying singlet state. While this singlet state (as obtained in a restricted Kohn–Sham formalism) has no biradicaloid nature, we examined a possible lower lying biradicaloid singlet structure by calculating an unrestricted singlet with the triplet wavefunction as the starting approximation. This led to the same energy and structure as in the restricted calculation, and hence the best description of **3** is homoaromatic (**3b**). To test whether the single-determinant Kohn–Sham and coupled-cluster schemes describe **3b** adequately, CAS(12,12) calculations on **3b** were performed. They revealed a squared weight of 0.84 for the configuration state function with the same occupation as the Kohn–Sham determinant, which indicates the absence of a multideterminant case here. Furthermore, the CASSCF calculations confirm that the ground-state multiplicity of **3b** is singlet. According to the CASSCF results the triplet state is more than 200 kJ mol<sup>-1</sup> higher in energy. Tetraphosphabarbaralane is thus homoaromatic, and Lewis structure **3b** is the best representation of the bonding situation.

By considering the HOMOs of the three barbaralanes, additional insight can be gained (Figure 3). Note that the HOMOs for each structure are plotted from different angles to give an optimal view.

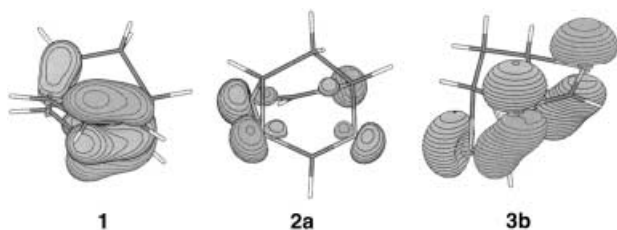


Figure 3. HOMOs of **1**, **2a**, and **3b**. The cyclopropane ring in **1** and **2a** is on the left-hand side.

The HOMO of **1** has two localized  $\pi$  orbitals at positions 3,4 and 6,7 as well as two  $sp^3$ - $p$   $\sigma$ -type orbitals at the cyclopropyl moiety. The frontier orbitals of **1** are mainly built from  $p$  atomic orbitals, while the frontier orbital region of **2a** and **3b** contains MOs of the lone pairs. The HOMO of **3b** deviates from that of **2a**, as **3b** shows a  $p_z$ - $p_z$ -like interaction without involvement of  $\sigma$  bonding (i.e., homoaromaticity). Tetraazabarbaralane **2a** and tetraphosphabarbaralane **3b** have in common that there is no contribution to the HOMO from the

atomic orbitals in positions 3 and 7. The ELF shown in Figure 4 facilitates further comprehension of the bonding situation.

In contrast to **1** and **2a** the phosphabarbaralane **3b** shows extensive basins that indicate extended lone pairs (double-headed arrow in Figure 4). The ELF isosurface can be

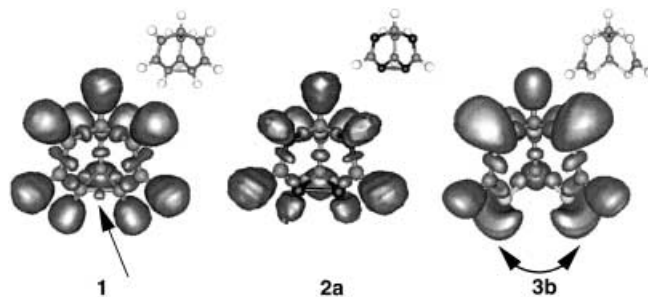


Figure 4. Isosurfaces for ELF = 0.85 of barbaralane (left), tetraazabarbaralane (middle), and tetraphosphabarbaralane (right).

increased up to a value of 0.99 for **3b** before it disappears at these lone pairs, whereas the lone pairs in **2a** already disappear at a value of 0.96. Both observations indicate highly localized lone pairs in the case of **3b** and hence a repulsive interaction between the P–P pairs which causes the long P–P distances. Further inspection reveals a bubblelike region of ELF on the C2–C8 bond in **1** (arrow in Figure 4). Such a bubble can only be obtained in the tetraazabarbaralane **2a** if the isosurface value is lowered to ELF = 0.72, and for the phosphorus compound **3b** no such bubble is observed. This indicates  $\sigma$ -type bonding at the 2,8-positions in **1** and in **2a**, but no such bonding in **3b**. Whereas the double bonds (dumbbell ELF) can be clearly distinguished from the single bonds (spherical ELF) in **1** and **2a**, **3b** has oval-like regions at all four bonds (positions 2-3, 3-4, 6-7, and 7-8), and this again indicates homoaromaticity.

To estimate the stability of the  $C_{2v}$ -symmetric barbaralane **3b**, we calculated the activation barrier for the Cope rearrangement of all three molecules together with the barrier of the experimentally known tetraazabarbaralane derivative **4a** (Figure 5). This molecule was used<sup>[7]</sup> to estimate an experimental value for the Cope barrier of the parent system **2a** by increment analysis, because the synthesis of **2a** might not be an easy task. For instance, instead of the sought-

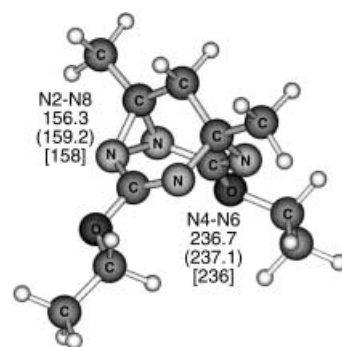


Figure 5. Minimum structure of **4a**. Distances are given for B3LYP/TZVP and BP86/TZVP (in parentheses) and compare very well with experimental data (in brackets).<sup>[13]</sup>

for tetraazasemibullvalene, 1,3,5,7-tetrazocines<sup>[12]</sup> were obtained.

For the  $C_s$ -symmetric barbaralanes **1** and **2a** a transition state was obtained on enforcement of  $C_{2v}$  symmetry. In the case of **4a** a transition state was found by increasing the N2–N8 distance stepwise in several constrained optimization procedures. For **3b** the “inverse barrier” can only be estimated from a  $C_s$ -distorted structure: We looked at the P–P distance of 1,2,3,4,5,6,7,8-octaphosphabarbaralane ( $P_8CH_2$ ), which has a  $C_s$  minimum structure (B3LYP/TZVP), and forced one P–P distance of **3b** to become, in a stepwise fashion, closer to the corresponding P–P bond length of the optimized  $C_s$ -symmetric  $P_8CH_2$ . Here, we also applied several constraint optimization procedures. The results of our calculations are given in Tables 1 and 2. Whereas in Table 1 only electronic energy differences  $\Delta E$  are listed, Table 2 lists the electronic energy differences with corrections for zero-point energy ( $\Delta D^+$ ) and enthalpies  $\Delta H^+$  at 298.15 K. Table 1 demonstrates how well the DFT methods perform in comparison to more accurate quantum chemical methods, while Table 2 serves for comparison with experimental data.

Table 1. Barrier heights  $\Delta E = E_{C_s}^{el} - E_{C_s}^{el}$  [kJ mol<sup>-1</sup>], obtained with different methods and basis sets. The  $C_s$ -symmetric structures were always taken as the zero-energy reference levels.

Compound	B3LYP		BP86/RI		MP2/RI		CCSD		CCSD(T)
	TZVP	TZVPP	TZVP	TZVPP	TZVP	TZVPP	SVP	TZVP	
<b>1</b>	28.5	28.6	19.7	20.0	17.7	13.5	64.0	56.9	48.6
<b>2</b>	14.0	14.2	3.8	4.5	-8.8	-11.6	43.1	45.7	16.6
<b>3</b>	-5.8	-5.9	-6.7	-5.7	-10.2	-14.1	-2.6	-2.8	-[a]
<b>4</b>	53.4	–	32.7	–	–	–	–	–	–

[a] See Methods of Calculation.

The DFT data in Table 1 indicate no strong dependency on the basis-set size. The BP86 functional systematically underestimates the B3LYP barriers by about 10 kJ mol<sup>-1</sup> but gives similar trends. Note that this systematic deviation does not occur for **3**, because the B3LYP  $C_s$ -symmetric structure was used for the corresponding BP86 single-point calculations. The MP2 calculation finds not only a  $C_{2v}$ -symmetric tetraphosphabarbaralane, but also a  $C_{2v}$ -symmetric tetraazabar-

baralane **2**. This MP2 result for **2** neither meets the predictions of all other methods nor the experimental findings for **4a**. The fact that the CCSD and CCSD(T) data (where available) are in reasonable agreement with the B3LYP data is very satisfying. It is unlikely that this agreement results from an error cancellation due to the smaller basis set used for the CCSD(T) calculations, because the CCSD calculations show that the barriers differ comparatively little with increasing basis-set size (i.e., from the SVP to the TZVP basis set). On the other hand, the correction caused by the perturbatively included triplets is much larger (cf. CCSD/SVP and CCSD(T)/SVP). This systematic investigation gives us the confidence to be able to describe all structures sufficiently accurately with DFT/B3LYP.

Table 2 compares our DFT data with experimental results. Whereas the B3LYP data for parent barbaralane **1** compare very well with experimental results, the agreement for the tetraazabarbaralane **2** is rather poor. This is not surprising, since several approximations were made to obtain the “experimental” value. To obtain this barrier we took an estimate of the increment from ref. [7], made for  $\Delta G^+$ , and added it to the experimental value of  $\Delta H^+$  from ref. [4].

However, for estimating the increment Moskau et al.<sup>[7]</sup> already made the following assumptions: 1) a methoxy is comparable to an ethoxy group, 2) methyl groups in positions 1 and 5 are negligible, 3) the situation in the semibullvalene is compared to the case of barbaralane, and 4) substitution at positions 3 and 7 is equivalent to substitution at positions 2 and 6. Alto-

gether the change in energy is in the correct direction, but it could be larger by a factor of two (see the extensive data collection in ref. [4]).

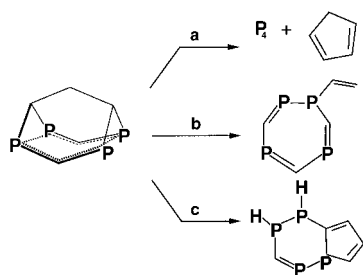
To circumvent the ambiguities of increment analysis in deriving experimental barriers we directly calculated the barrier of **4a**, which Moskau et al.<sup>[7]</sup> measured in NMR experiments. We restricted ourselves to DFT calculations with the TZVP basis set, which have proven to be sufficiently accurate. The B3LYP/TZVP value for  $\Delta H^+$  (44.3 kJ mol<sup>-1</sup>) is in good agreement with the experimental value (41.6 kJ mol<sup>-1</sup>). Again the BP86/TZVP barrier is more than 10 kJ mol<sup>-1</sup> lower, which is consistent with our findings for **1** and **2**.

Another way to examine the stability of the symmetrical tetraphosphabarbaralane **3b** is to consider its decomposition reactions. Decomposition to  $P_4$  and cyclopentadiene (Scheme 1, path a) is assumed to be the thermodynamic sink. We found that these two molecules are only about 150 kJ mol<sup>-1</sup> more stable than 2,4,6,8-tetraphosphabarbaralane (see Table 3). However, this is not a good estimate for molecules that possibly serve as starting materials for the synthesis of **3b** or which result from rearrangement of **3b**. Therefore, we also calculated the decomposition to give a retro-Diels–Alder product (i.e., a tetraphosphadervative of 7-vinyl-1,3,5-cycloheptatriene, path b), and the formation of a dihydroindene derivative (path c).

Table 2. Barrier heights  $\Delta D^+ = D_{0,C_{2v}} - D_{0,C_s}$  (0 K) and  $\Delta H^+ = H_{C_{2v}}^{298} - H_{C_s}^{298}$  [kJ mol<sup>-1</sup>] (298.15 K). The  $C_s$ -symmetric structures were always taken as the zero-energy reference levels.

Compound	B3LYP		BP86/RI		exp.	
	TZVP	TZVPP	TZVP	TZVPP	$\Delta D^+$	$\Delta H^+$
<b>1</b>	27.5	29.2	24.4	26.7	16.4	18.5
<b>2</b>	11.7	13.6	13.1	14.8	3.7	4.7
<b>3</b>	-5.8	-5.8	-5.1	-4.8	-8.5	-8.6
<b>4</b>	44.3	44.3	–	–	23.3	27.8

[a] This value was obtained by adding an increment for the  $\Delta G^+$  value of parent barbaralane to its  $\Delta H^+$  value. The increment was estimated by the authors of ref. [7] to obtain a value for the barrier of structure **2a** from that of **4a**.



Scheme 1. Possible decomposition reactions of tetraphosphabarbaralane.

Table 3. Energies [kJ mol<sup>-1</sup>] for the model decomposition reactions a–c in Scheme 1, calculated with B3LYP/TZVPP.  $\Delta E$  denotes the electronic energy difference,  $\Delta D_0$  also includes the zero-point vibrational energies, and  $\Delta H$  at 298.15 K is the enthalpy calculated within the harmonic force-field approximation.

reaction	$\Delta E$	$\Delta D_0$	$\Delta H$
a	-146.2	-148.4	-159.5
b	120.9	107.6	112.9
c	10.1	-5.5	-3.4

The reaction energies and enthalpies for the decomposition reactions a, b, and c are given in Table 3. While the cycloheptatriene derivative in reaction b is more than 100 kJ mol<sup>-1</sup> less stable than **3b**, the dihydroindene compound in reaction c is of similar stability to **3b**. Because the activation barrier for decomposition reaction c may be high due to the extensive rearrangement of the molecular  $\sigma$ -bonded skeleton, we assume that tetraphosphabarbaralane is a feasible synthetic target.

Apart from X-ray structure analysis, vibrational spectroscopy could be an important experimental tool for identification of **3b**. From the calculated IR line spectrum of **3b**, compared with that of **1** in Figure 6, four characteristic intensive normal modes can be identified at 582, 825, 976, and 1264 cm<sup>-1</sup>. These may serve as diagnostic bands in an experimental spectrum.

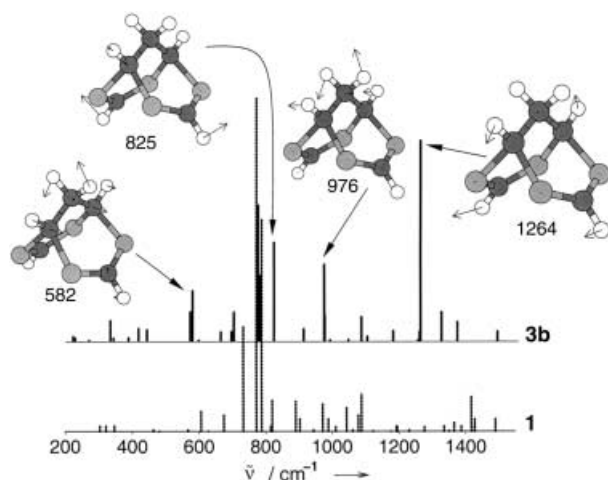


Figure 6. Characteristic normal vibrations of  $C_{2v}$ -symmetric tetraphosphabarbaralane (top) and barbaralane (bottom). Wavenumbers are given in cm<sup>-1</sup> (B3LYP/TZVPP). Each normal mode is indicated by small arrows on the atoms of the molecule.

In ref. [5] the authors write “There remains the dearth of neutral homoaromatics.” and further: “Quast reports observing vibronically excited homoaromatic semibullvalene and barbaralanes under ordinary condition. Even more exciting is his evidence for homoaromatic semibullvalenes and barbaralanes being of lower energy than the corresponding localized forms in highly dipolar solvents. Surely ground-state homoaromatic semibullvalenes and barbaralanes cannot be far away.”

Tetraphosphabarbaralane is such a symmetrical barbaralane. Our study demonstrates that barbaralanes become the more symmetrical the heavier the heteroatoms in positions 2,4,6,8 are. In the case of phosphorus, we found a fully symmetrical ground state, that is, we have presented the first example of a neutral  $C_{2v}$ -symmetric ground-state barbaralane at zero temperature. We tested **3b** against decomposition and could show it is even stable from a purely thermodynamic viewpoint. Now we would like to let the experimentalists take their turn and see whether 2,4,6,8-tetraphosphabarbaralane is stable under laboratory conditions.

### Methods of Calculation

We employed DFT with the functional BP86<sup>[16,17]</sup> and the hybrid functional B3LYP<sup>[18,19]</sup>, second-order Møller–Plesset (MP2) perturbation theory, the coupled-cluster models CCSD and CCSD(T), and multiconfiguration SCF calculations with CAS(12,12) to gain a consistent picture independent of the method, although systematic investigations of organophosphorus compounds were already undertaken by Nguyen et al. The main conclusion of their broad study was that “the B3LYP method, when employed with a large basis set, yields energetic results comparable to the CCSD(T) results”.<sup>[20]</sup> In addition, several studies could show the excellent agreement of the B3LYP with the CCSD(T) method for the Cope rearrangement of many different molecules, including bullvalenes; see ref. [21] and references therein. The CCSD(T) calculations are needed to support the other methods, as such calculations lack exact exchange (DFT/BP86), non-dynamical correlation (DFT/BP86, DFT/B3LYP), and dynamical correlation (CASSCF). As the CASSCF calculations are able to confirm whether the electronic structure of a molecule is dominated by a single configuration but otherwise are less accurate than CCSD and CCSD(T), they were used for this purpose only. The all-electron DFT calculations and MP2 calculations were carried out with the programs provided by the Turbomole 5.1 suite.<sup>[22]</sup> For the MP2<sup>[23]</sup> and the BP86<sup>[24,25]</sup> calculations the resolution-of-identity (RI) technique was applied. Ahlrichs’s TZVPP basis set (i.e., TZV kernel<sup>[26]</sup> + polarization functions from Dunning’s cc-pVTZ, as implemented in Turbomole) was used for DFT and MP2 calculations. To demonstrate the basis-set dependence, we also report TZVP results.

The CCSD(T) and CASSCF calculations were performed with the program Dalton<sup>[27]</sup> on the B3LYP optimized structures. Since the TZVPP basis set is too large to sustain such correlation methods we employed Ahlrichs’s SVP and TZVP basis sets.<sup>[26,28]</sup> Furthermore, tetraphosphabarbaralane is beyond the scope of current standard CCSD(T) calculations, as it is known<sup>[29]</sup> that at least triple-zeta basis sets must be used. This situation is complicated further by the fact that a frozen-core approximation can hardly be applied, because test calculations have revealed that at most the energetically lowest lying four molecular orbitals can be frozen.

All frequency analyses were performed within the harmonic approximation with the SNF program package<sup>[30,31]</sup> as numerical first derivatives of analytical gradients of the total electronic energy obtained from Turbomole. The electron localization function (ELF), which we utilize for understanding electronic structure, is a measure of the spherically averaged Fermi hole around a reference electron.<sup>[32]</sup> It is mapped onto an interval  $0 < \text{ELF} < 1$ .  $\text{ELF} \approx 1$  indicates areas of a localized exchange potential, where electrons are highly localized.

Received: February 7, 2002  
Revised: May 28, 2002 [Z18666]

- [1] W. von E. Doering, W. R. Roth, *Angew. Chem.* **1963**, 75, 27–35; *Angew. Chem. Int. Ed. Engl.* **1963**, 2, 115–122.
- [2] R. Hoffmann, W.-D. Stohrer, *J. Am. Chem. Soc.* **1971**, 93, 6941–6948.
- [3] M. J. S. Dewar, D. H. Lo, *J. Am. Chem. Soc.* **1971**, 93, 7201–7207.
- [4] L. M. Jackman, E. Fernandes, M. Heubes, H. Quast, *Eur. J. Org. Chem.* **1998**, 2209–2227.
- [5] R. V. Williams, *Chem. Rev.* **2001**, 101, 1185–1204.
- [6] R. Trinks, K. Müllen, *Chem. Ber.* **1987**, 120, 1481–1490.
- [7] D. Moskau, W. Leber, H. Günther, R. Gompfer, P. Spes, *Chem. Ber.* **1989**, 122, 2361–2364.
- [8] C. Schnieders, H.-J. Altenbach, K. Müllen, *Angew. Chem.* **1982**, 94, 638–639; *Angew. Chem. Int. Ed. Engl.* **1982**, 21, 637–638; *Angew. Chem. Suppl.* **1982**, 1353–1359.
- [9] M. Baudler, *Angew. Chem.* **1982**, 94, 520–539; *Angew. Chem. Int. Ed. Engl.* **1982**, 21, 492–512.
- [10] D. Schröder, H. Schwarz, M. Wulf, H. Sievers, P. Jutzi, M. Reiher, *Angew. Chem.* **1999**, 111, 3723–3726; *Angew. Chem. Int. Ed.* **1999**, 38, 3513–3515.
- [11] M. Häser, O. Treutler, *J. Chem. Phys.* **1995**, 102, 3703–3711.
- [12] R. Gompfer, H.-U. Wagner, *Angew. Chem.* **1988**, 100, 1492–1511; *Angew. Chem. Int. Ed. Engl.* **1988**, 27, 1437–1455.
- [13] R. Gompfer, H. Nöth, P. Spes, *Tetrahedron Lett.* **1988**, 29, 3639–3642.
- [14] H. Günther, J. Runsink, H. Schmickler, P. Schmitt, *J. Org. Chem.* **1985**, 50, 289–293.
- [15] H. Baumann, A. Voellinger-Borel, *Helv. Chim. Acta* **1997**, 80, 2112–2123.
- [16] A. D. Becke, *Phys. Rev. A* **1988**, 38, 3098–3100.
- [17] J. P. Perdew, *Phys. Rev. B* **1986**, 33, 8822–8824.
- [18] A. D. Becke, *J. Chem. Phys.* **1993**, 98, 5648–5652.
- [19] P. J. Stephens, F. J. Devlin, C. F. Chabalowski, M. J. Frisch, *J. Phys. Chem.* **1994**, 98, 11623–11627.
- [20] M. T. Nguyen, S. Creve, L. G. Vanquickenborne, *J. Chem. Phys.* **1996**, 105, 1922–1932.
- [21] D. A. Hrovat, R. V. Williams, A. C. Goren, W. Thatcher Borden, *J. Comput. Chem.* **2001**, 22, 1565–1573.
- [22] R. Ahlrichs, M. Bär, M. Häser, H. Horn, C. Kölmel, *Chem. Phys. Lett.* **1989**, 162, 165–169.
- [23] F. Weigend, M. Häser, H. Patzelt, R. Ahlrichs, *Chem. Phys. Lett.* **1998**, 294, 143–152.
- [24] K. Eichkorn, O. Treutler, H. Öhm, M. Häser, R. Ahlrichs, *Chem. Phys. Lett.* **1995**, 240, 283–290.
- [25] K. Eichkorn, F. Weigend, O. Treutler, R. Ahlrichs, *Theor. Chem. Acc.* **1997**, 97, 119–124.
- [26] A. Schäfer, C. Huber, R. Ahlrichs, *J. Chem. Phys.* **1994**, 100, 5829–5835.
- [27] T. Helgaker, H. J. Aa. Jensen, P. Jørgensen, J. Olsen, K. Ruud, H. Ågren, A. A. Auer, K. L. Bak, V. Bakken, O. Christiansen, S. Coriani, P. Dahle, E. K. Dalskov, T. Enevoldsen, B. Fernandez, C. Hättig, K. Hald, A. Halkier, H. Heiberg, H. Hettema, D. Jonsson, S. Kirpekar, R. Kobayashi, H. Koch, K. V. Mikkelsen, P. Norman, M. J. Packer, T. B. Pedersen, T. A. Ruden, A. Sanchez, T. Saue, S. P. A. Sauer, B. Schimmelpfennig, K. O. Sylvester-Hvid, P. R. Taylor, O. Vahtras, DALTON, a molecular electronic structure program, Release 1.2, **2001**.
- [28] A. Schäfer, H. Horn, R. Ahlrichs, *J. Chem. Phys.* **1992**, 97, 2571–2577.
- [29] T. Helgaker, J. Gauss, P. Jørgensen, J. Olsen, *J. Chem. Phys.* **1997**, 106, 6430–6440.
- [30] C. Kind, M. Reiher, J. Neugebauer, B. A. Hess, SNF, University of Erlangen-Nürnberg, **1999–2001**.
- [31] J. Neugebauer, M. Reiher, C. Kind, B. A. Hess, *J. Comput. Chem.* **2002**, 23, 895–910.
- [32] A. D. Becke, K. E. Edgecombe, *J. Chem. Phys.* **1990**, 92, 5397–5403.

## A Highly Reactive Uranium Complex Supported by the Calix[4]tetrapyrrole Tetraanion Affording Dinitrogen Cleavage, Solvent Deoxygenation, and Polysilanol Depolymerization\*\*

Ilia Korobkov, Sandro Gambarotta,\* and Glenn P. A. Yap

Pyrrole-based polyanions are versatile ligands for *f* block metals which have been proved capable of assembling large cluster structures and of substantially increasing the reactivity of their low-valent derivatives. This is especially evident in the chemistry of divalent samarium, where the utilization of tetra- and dipyrrolyl anions leads to a larger extent of dinitrogen reduction through interaction with four metal centers.<sup>[1,2]</sup> However, a complete breakage of the N–N bond, as observed in transition-metal chemistry,<sup>[3]</sup> has not been observed in lanthanide chemistry, despite the possibility of assembling high-nuclearity low-valent clusters.<sup>[4]</sup>

Trivalent and lower valence uranium complexes might be promising substrates for N<sub>2</sub>-activation purposes. For example, trisamide derivatives have recently provided the first two examples of dinitrogen fixation in actinide chemistry,<sup>[5]</sup> while the only existing complex of a formally divalent uranium amide displays a rare  $\mu, \pi$  coordination of toluene.<sup>[6]</sup> These studies suggest that a high level of reactivity may be expected for low-valent uranium compounds with N-donor-based ligands. In addition, the possibility of uranium exhibiting several oxidation states and of affording multielectron reductions makes its low-valent derivatives particularly desirable. Accordingly, a preliminary study has shown that a trivalent uranium tetrapyrrolyl complex may perform different types of solvent fragmentation, C–H bond oxidative addition, and ligand isomerization.<sup>[7]</sup>

Herein, we describe the results of our attempts to prepare a highly reduced uranium complex, which results in a surprising variety of processes including dinitrogen cleavage, solvent deoxygenation, and polysilanol depolymerization.

The starting complex [(Et<sub>8</sub>-calix[4]tetrapyrrole)U(dme)][K(dme)] (**1**, DME = 1,2-dimethoxyethane) was synthesized by using the procedure previously reported for the preparation of the cyclohexyl congener<sup>[7]</sup> by the direct reaction of [UI<sub>3</sub>(dme)<sub>2</sub>] with the tetrapotassium salt of the Et<sub>8</sub>-calix[4]-tetrapyrrole ligand (Scheme 1). The crystalline compound, isolated upon cooling the solution in DME, was characterized by X-ray crystallography (see Supporting Information) and standard analytical techniques.

[\*] Prof. S. Gambarotta, Dr. I. Korobkov, Dr. G. P. A. Yap  
Department of Chemistry  
University of Ottawa  
Ottawa, ON, K1N 6N5 (Canada)  
Fax: (+1) 613-5672-5170  
E-mail: sgambaro@science.uottawa.ca.

[\*\*] This work was supported by the Natural Sciences and Engineering Council of Canada (NSERC) and by NATO (travel grant). We thank Dr. Viktor Tersikh (NRC Ottawa) and Dr. P. Tregenna-Piggott (University of Bern) for assistance with recording and interpreting ESR spectra.